

# VALIDATION OF SPATIAL AUTOCORRELATION METHOD WITH L-SHAPE ARRAY IN JYOSO CITY, JAPAN

Prithvi Lal SHRESTHA\*  
MEE09182

Supervisor: Toshiaki YOKOI\*\*

## ABSTRACT

This study is aimed to validate the efficiency of an L-shape array for SPAC method using microtremor in estimating the shear wave velocity ( $V_s$ ) structure. The experiment for validation was conducted in the Toyota Community Baseball Ground, Jyoso City, Ibaraki Prefecture, Japan in March 2009 with an equilateral triangle array with side length of 40m and in June 2010 with an equilateral triangle array with side length of 50m, together with an L-shape array of the similar size. Multichannel Analysis of Surface Waves (MASW) was also performed simultaneously in June 2010. In the same lot PS-logging data are available from nearby IBRH10 station of the KIK-NET (NIED, Japan) that shows soft sediment of about 20m thick with  $V_s$  of 110 m/s in the geological column of the site.

The comparison of the determined phase velocity and that calculated from PS logging data shows close matching of two sets of curves separately. One is between PS logging and the triangle array (40m) and the other is between the triangle array (50m) and the L-shape array (50m). Former two are of the almost same place whereas other two arrays are deployed about 200m away from the other set. Some discrepancy between two sets is shown. This seems due to lateral variation of underground velocity structure which is consistent with the result of MASW.

Based on the results of analysis we can say that an L-shape array can be applied to estimate shear wave velocity for shallow depth so it can be layout in urban areas to determine phase velocity information from microtremor. Therefore it may be feasible to apply it in the Kathmandu valley, Nepal that is based upon the soft soil with high possibility of liquefaction or earthquake hazard.

**Keywords:** SPAC, PS logging data, Equilateral Triangle array, L-shape array.

## 1. INTRODUCTION

Nepal Himalaya lies in the active seismic belt. Seismicity in the Himalaya is the consequence of under-thrusting of the Indian plate towards the north lying Tibetan plate. Nepal has suffered earthquake disasters through its history due to its high seismicity and highly vulnerable construction practices, therefore one of the most earthquake disaster prone countries in the world.

### 1.1. Purpose of my study

Since we are expecting a great earthquake disaster in near future in our country Nepal, seismic hazard assessment is required. Estimation of the amplification factor of the ground, i.e., microzonation on the basis of the shallow  $V_s$  structure is a basic step of seismic hazard assessment. The microtremor array measurement will be applied in Nepal in future, because this SPAC method seems to be reliable, easy

---

\*National Seismological Centre, Department of Mines & Geology, Kathmandu, Nepal.

\*\*Chief Research Scientist, International Institute of Seismology and Earthquake Engineering, BRI, Japan.

to handle, comparatively affordable and do not cause any environmental problems, thus suitable as a tool for seismic microzonation and earthquake disaster mitigation.

Conventional circular or equilateral triangle arrays, however, are sometimes difficult to deploy in crowded urban areas where only L-shape or linear arrays layout can suit to road pattern. The purpose of this study is to understand the effectiveness, limitations and advantages of L-shape array for the SPAC method by applying and verifying the applicability and accuracy by comparison with standard equilateral triangle array in Jyoso city, Ibaraki, Japan.

## 2. METHODOLOGY

### 2.1. SPAC method

This is a successful method to determine the phase velocity information from surface waves contained in microtremor (e.g., Aki 1957; Okada 2003). The SPAC coefficient for distance  $r$  between two stations at the angular frequency  $\omega$  provides the information about the phase velocity of the propagating waves in the array. This is obtained by the azimuthal average of coherency between microtremor records observed at two stations.

$$\rho(\omega, r) = J_0\left(\frac{\omega r}{c(\omega)}\right) = \frac{1}{2\pi} \int_0^{2\pi} \frac{\text{Re}[S_{cx}(\omega; r, \theta)]}{\sqrt{S_{cc}(\omega; 0, 0)S_{xx}(\omega, r, \theta)}} d\theta, \quad (1)$$

where,  $J_0(\cdot)$  is the Bessel function of the first kind with zero order,  $c(\omega)$  is the phase velocity ( $\omega=2\pi f$ ).

### 2.2. New interpretation

Shiraishi et al. (2006) proposed the following formula using a mathematical relationship between  $\cos(x\cos\theta)$  and the Bessel function of the first kind,

$$\text{Re}(\gamma_{pq}) = J_0\left(\frac{\omega r}{c(\omega)}\right) + 2 \sum_{n=1}^{\infty} \{(-1)^n J_{2n}\left(\frac{\omega r}{c(\omega)}\right) \sum_{l=1}^L \lambda_l \cos 2n\theta_l\}, \quad (2)$$

where,  $\text{Re}(\gamma_{pq})$  is equal to the integrand of the third member of Eq.(1), namely the coherency,  $L$  is the number of wave sources,  $\lambda_l$  is rate of the contribution of the  $l$ -th wave source to the power spectra at the observation point,

$\theta_l$  is azimuth of the  $l$ -th wave source,  $J_m(\cdot)$  is  $m$ -th order Bessel function of first kind. Here  $J_0(\omega r/c(\omega))$  is already included in the integrand. The application of L-shape array relies on this formula. L-shape array has error of the 4th and higher order Bessel functions as follows.

$$\rho_L(\omega r_{01}) = \frac{\text{Re}\{\gamma_{z,01}\} + \text{Re}\{\gamma_{z,02}\}}{2} = J_0\left(\frac{\omega r_{01}}{c(\omega)}\right) + J_4\left(\frac{\omega r_{01}}{c(\omega)}\right) \left\{ 2 \sum_{l=1}^L \lambda_l \cos 4\theta_l \right\} + O\left(J_8\left(\frac{\omega r_{01}}{c(\omega)}\right)\right). \quad (3)$$

Equilateral triangle array averages out the terms of  $J_2(\cdot)$  and  $J_4(\cdot)$ , whereas L-shape array cancels out the term of  $J_2(\cdot)$  only. Therefore, L-shape array seems weaker against undesirable azimuth dependent noise contained in microtremor. From Eq.(3), it is expected that the average over two pairs that form the short sides can reduce the influence of  $J_2(\cdot)$  term drastically, whereas the oblique sides follow Eq.(2). Therefore it is better to eliminate the oblique sides from the analysis.

### 2.3. Procedure of analysis

Triangle and L-shape arrays are set up to get the microtremor data (Figure 1). First SPAC coefficient is obtained after filtering and resampling and then screening is done. Second, the dispersion curve of Rayleigh wave is determined and finally velocity structure model is estimated by the heuristic search method using the very fast simulated annealing method (VFSA) combined with the downhill simplex method (DHSM) (VFSA-DHSM, Yokoi 2005).

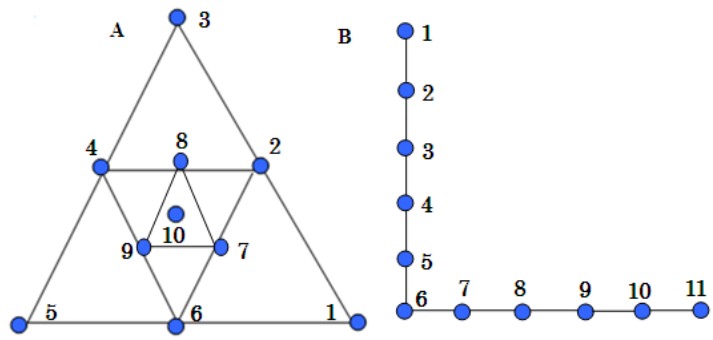


Figure 1. Schematic figures of A) equilateral triangle array and B) L-shape array.

## 3. DATA ACQUISITION

### 3.1. Observation site

The experiment was conducted in the Toyota Community Baseball Ground, Jyoso City, Ibaraki Prefecture, Japan in March 2009 and June 2010. IBRH10 of KIK-NET (NIED, Japan) is located at the south-east corner of the same lot where PS-logging data are available. MASW (Hayashi and Suzuki 2004) was also conducted this year. Soft sediment as thick as about 20 m with velocity of S-wave ( $V_s$ ) 110 m/s is observed in the geological column at IBRH10. There are a national road R294 about 300 m west and a prefectural road 24 about 100 m south and both of them have heavy traffic all day long (Figure 2).

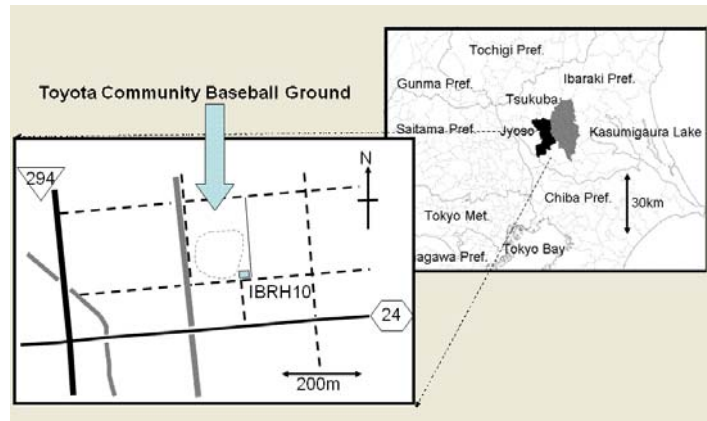


Figure 2. Location map of measurement site (Yokoi and Hayashi 2009).

The baseball ground itself, however, was almost quiet during the measurement (Yokoi and Hayashi 2009).

### 3.2. Array deployment and instruments

Equilateral triangle array with side length of 40m with 7 sensors was deployed in March 2009 nearby IBRH10 whereas 50 m of equilateral triangle with 10 sensors and L-shape array with 11 sensors were deployed in June 2010 about 200m away from IBRH10. All sensors are vertical component. MASW with total length of 105m was conducted in the same place.

## 4. ANALYSIS AND RESULTS

### 4.1. Preprocessing

Multiplexing and re-sampling are done applying digital anti-aliasing filter (Saito 1978). The screening is conducted next with two steps. The data are divided into time blocks with 512 samples. The consecutive time blocks are overlapped each other by 50% of their duration.

First step: If peak is greater than “*ajudge*” times of RMS amplitude then this time block is not used in analysis. This is a countermeasure against impulsive noise due to traffic, i.e. vehicles passing near by sensors.

Second step: If RMS amplitude in a time block deviates more than another given constant “*a\_sgm*” times the standard deviation from the average, this time block is not used in analysis, where the average and the standard deviation are calculated over the all time blocks that survived in the above mentioned screening step 1. This is a countermeasure against outliers.

In this study *ajudge*=4 and *a\_sgm*=2 are used for the screening of the obtained data.

### 4.2. SPAC coefficient calculation

Re-sampled and screened time block files are used to calculate SPAC coefficient that is an azimuthal average of the coherency between microtremor records at two stations. The initial frequency range of analysis is set from 0.1Hz to 10Hz. Band width of Parzen window for smoothing power and cross spectra is set at 0.5Hz.

Figure 3 A) shows the SPAC coefficient of station pairs that compose the 50m triangle array and B) shows SPAC coefficient with its standard deviation of the 50m triangle array (inter-station distance 25m). It is clear that for the shorter distances the first positive lobe of SPAC coefficient shows higher values and has wider range of frequencies. It is also clearly seen that SPAC coefficient is decreasing at low frequency side but theoretically it should reach 1 at the frequency 0.0Hz.

This variation is due to the available frequency range of seismometer. For Figure 3 the natural frequency of the used seismometers is 2Hz.

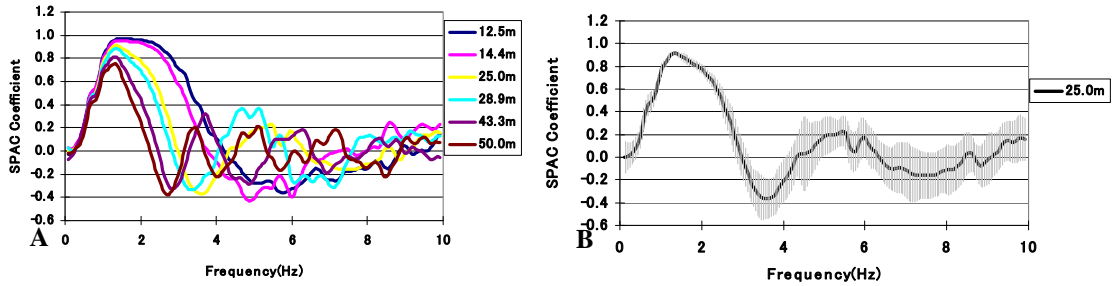


Figure 3. SPAC coefficients: A) Those of the station pairs that compose the 50m triangular, B) of the 50m triangular array (inter-station distance 25m).

### 4.3. Determination of dispersion curve

The dispersion curve of Rayleigh wave i.e., the phase velocity depending upon the frequency is determined from SPAC coefficient. First, SPAC coefficient  $\rho(\omega r)$  is converted to the value of  $kr$  by applying the following fifth order polynomial equation that approximates the inverse function of  $J_0(kr)$  from  $kr = 0.0$  to the first trough of  $J_0(kr)$ . If  $x = J_0(y)$ ,

$$y \approx -6.0803x^5 + 9.2477x^4 - 3.9322x^3 + 0.1815x^2 - 1.7079x + 2.4121 \quad (4)$$

The first maximum of  $c(\omega)$  from the low frequency side is recognized as a lower limit of the available frequency range for the respective inter-station distance. The maximum from this lower limit to the highest one is recognized as the high frequency limit of the available frequency range. Then these values again are averaged and converted to  $c(\omega) = r\omega/(kr)$ . The weight coefficient used at averaging is the reciprocal of the variance of SPAC coefficients at the respective inter-station distance and the frequency.

#### 4.4. Estimation of velocity structure by Heuristic search

A heuristic search method is conducted to obtain the optimum underground structure by fitting the theoretical phase velocity of Rayleigh wave to the observed dispersion curve. Five layer models are introduced with its search range. The used method is the downhill simplex method (DHSM, e.g., Press et al. 2002) combined with the very fast simulated annealing (VFSA, Ingber 1989). Hereafter, the combined methods is called the DHSM-VFSA. The optimum, namely, the fastest schedule for the inversion of underground velocity structure from the dispersion curve of Rayleigh waves is used with the parameters  $t_0=1.0$ ,  $a=0.6$ , and  $c=1.3$  as given by Yokoi (2005).

### 5. DISCUSSION

#### 5.1. Comparison of dispersion curves

Figure 4 shows a comparison of phase velocity over frequency between 40m triangle, 50m triangle and 50m L-shape arrays with the curve of PS logging data. This shows close matching of two sets of curves separately, one is between PS logging and 40m triangle and the other is 50m triangle and L-shape. PS logging and 40m triangle array are from the same place where other two arrays are also from the same place but about 200m away from the other set. A discrepancy is seen between these two sets. This seems to be due to lateral variation of underground velocity structure as MASW result implies.

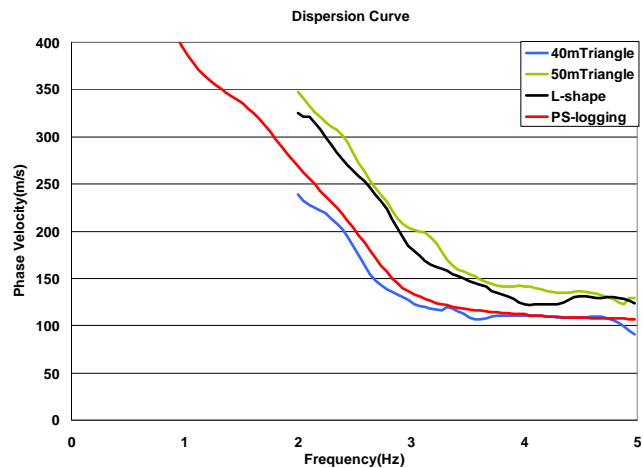


Figure 4. Comparison of the dispersion curves with PS logging data.

#### 5.2. Comparison of velocity structure

Figure 5 shows the comparison of  $V_s$  structure models determined by the data of the three arrays with the PS logging data.  $V_p$  is fixed to 1500m/s for the 1st to 4th layer and 1956m/s for the underlying half space. Density is calculated from  $V_p$  then fixed to  $1.9\text{g/cm}^3$  and  $2.13\text{g/cm}^3$  respectively (Ludwig et al. 1970). As seismometer's natural frequency is 2.0Hz, the lower limit of the frequency range for analysis is set at 2.0Hz and the upper one at 5.0Hz by considering on the S/N of microtremor. The value of misfit is as small as 3.0, 4.0 and 4.2

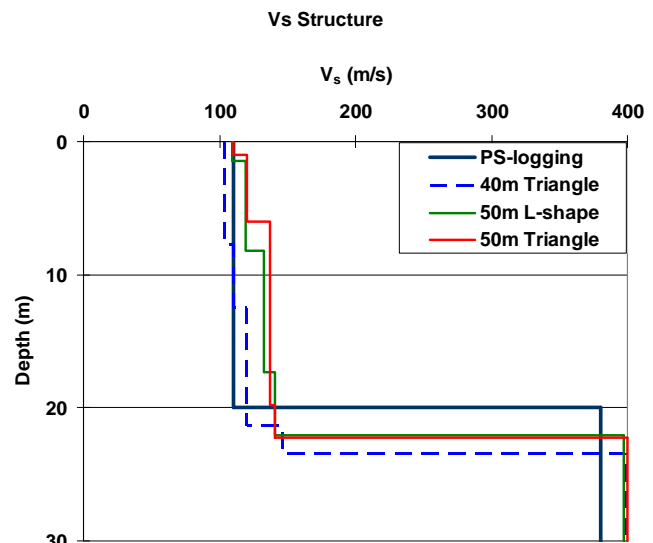


Figure 5. Comparison of velocity structures with PS-logging data

m/s for the triangular array (40m), triangular array (50m) and L-shape array respectively.

From Figure 5 it is clear that for the 20m depth  $V_s$  of all arrays are similar to the logging data i.e., around 110m/s to 150m/s that implies soft soil.  $V_s$  structures of the triangular array (50m) and L-shape array coincide to each other whereas 40m triangle shows a clear deviation from them and lower  $V_s$  than PS logging data. This shows that the lateral variation of underground velocity structure implied by MASW is detected also using SPAC method.

## 6. CONCLUSION

In this study I have conducted the analysis of the data of microtremor array observation held in the Toyota Community Baseball Ground, Jyoso city, Ibaraki prefecture, Japan for shallow depth using L-shape and equilateral triangle array with the SPAC method for Rayleigh wave in comparison with PS logging data and MASW. The dispersion curve and  $V_s$  Structures determined by the data of L-shape array coincide well to those of equilateral triangular array (50m). These deviate together from  $V_s$  structure of PS logging data and the dispersion curve calculated from PS logging data respectively. This discrepancy, however, is due to lateral variation of  $V_s$  structure as the result of the triangular array (40m) shows and that of MASW implies. Based on the results of analysis I conclude that L-shape array can be applied to estimate  $V_s$  structure for shallow depth so it can be layout in urban areas to determine phase velocity information from surface wave in microtremor.

## ACKNOWLEDGEMENT

I would like to express my sincere gratitude to Dr. Koichi Hayashi, OYO Corporation for his help during the field work.

## REFERENCES

- Aki, K., 1957, Bulletin of Earthquake Research Institute, 35, 415-457.
- Hayashi, K., and Suzuki, H., 2004, Exploration Geophysics, 35, 7-13.
- Ingber, L., 1989, Mathematical and Computer Modeling, 12, 967-973.
- Ludwig, W. J. et al., 1972, The Sea, Vol. 4, Wiley-Interscience, New York, 53-84
- Okada, H., 2003, The Microtremor Survey Method. Society of exploration geophysicists.
- Press, W. H., et al., 2002, Numerical recipes. Cambridge University Press.
- Saito, M., 1978, BUTURI- TANSU, 31, 112-135 (in Japanese with English abstract).
- Shiraishi, H., et al., 2006, Geophys. Res Let, Vol. 33, L18307.
- Yamanaka, H., 2004, Proc. of 13th World Conference on Earthquake Engineering, Paper 1161.
- Yokoi, T., 2005, Programme and Abstract, Seismological Society of Japan Fall Meeting, B049.
- Yokoi, T., and Hayashi, K., 2009, Proc. of 9th Int. WS on Seismic Microzoning and Risk Reduction, Cuernavaca, Mexico.